Electronic Ground States of Iron Porphyrin and of the First Species in the Catalytic Reaction Cycle of Cytochrome P450s

André R. Groenhof, Marcel Swart, Andreas W. Ehlers, and Koop Lammertsma*

Department of Chemistry, Vrije Universiteit, FEW, De Boelelaan 1083, 1081 HV Amsterdam, The Netherlands

Received: December 23, 2004; In Final Form: February 4, 2005

Electronic structures of iron(II) and iron(III) porphyrins are studied with density functional theory (DFT) using the GGA exchange functional OPTX in combination with the correlation functional PBE (OPBE) and with the correlation functional Perdew (OPerdew) together with a triple ζ-type basis set. These functionals, known for accurately predicting the spin ground state of iron complexes, are evaluated against other functionals for their performance in calculating relative energies for the various electronic states of both the iron porphyrins. The calculated energy orderings are triplet < quintet < singlet for the iron(II) porphyrin and quartet < sextet < doublet for the iron(III) porphyrin cation. Complexation by a thiolate ion (SH^-) changes the preferred ground state for both species to high spin. This thiolate complex is used as a mimic for the cytochrome P450s active site to model the first step of the catalytic cycle of this enzyme. This first step is believed to concern the removal of an axial oxygen donating ligand from the hexacoordinated aqua-thiolate-porphyrin-iron(III) resting state. The DFT results suggest that this is not a free water molecule, because of its repulsive nature, but that it has instead hydroxy anion character. These calculations are in line with the experimentally observed change in the spin state from low to high spin upon this removal of the axial hydroxo ligand by binding of the substrate in the heme pocket of cytochrome P450.

Introduction

Iron porphyrins play an important role in biological systems as the active centers or prosthetic groups of heme-proteins.[1] Cytochrome P450s, for example, are a ubiquitous family of metabolizing heme-thiolate enzymes with more than 500 known isoenzymes.[2] These cytochromes mainly catalyze the monooxygenation of a variety of hydrophobic substrates.[2,3] This is a two-electron oxidation of the substrate in which one of the oxygen atoms from dioxygen is inserted into the C−H bond of the substrate.[2,3] Most P450 enzymes share similar chemistry and therefore enable a general description of the catalytic reaction cycle (summarized in Figure 1). This cycle has been subject to intense experimental and computational mechanistic studies, including combined quantum mechanical/molecular mechanics (QM/MM) methods, because of lingering questions about various reaction steps.[1−21] In the present study, we address the first steps of the catalytic cycle using a density functional theory approach.

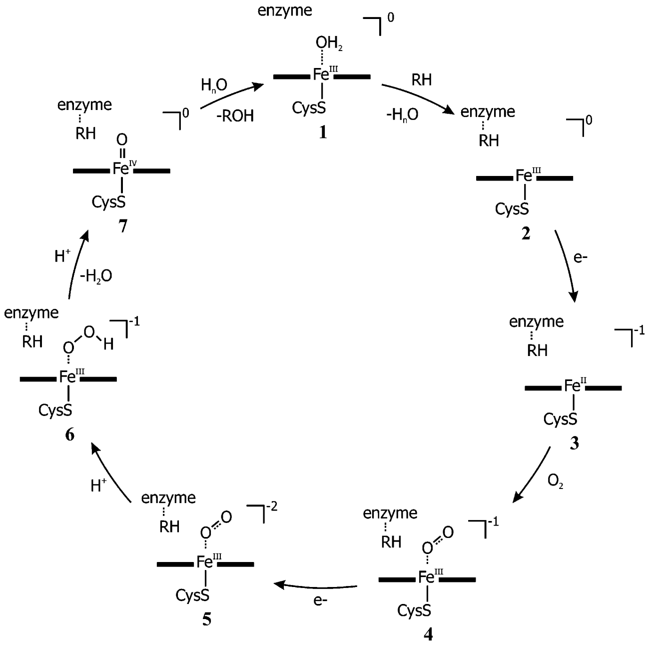

Figure 1. Cytochrome P450 catalytic reaction cycle. RH represents the substrate, ROH the product, and −Fe− the iron protoporphyrin IX.

The active site of the cycle is composed of an iron(III) protoporphyrin(IX) moiety with a cysteine amino acid from the protein backbone as an axial ligand to the iron. In the resting state **1**, a water molecule is the second axial ligand bound to the iron. The cycle is initiated by substrate binding to the iron(III) P450 active site (**1**) accompanied by the displacement of the axial water molecule. Subsequently, the P450 redox partner, which may either be an iron−sulfur redoxin, a flavoprotein, or cytochrome b_5, depending on the particular P450 enzyme, reduces the iron(III) heme (**2**) to the iron(II) state (**3**). Oxygen binding leads to an iron(III)−superoxide species (**4**) after which a second electron is transferred from a redox partner to this oxy-P450 species (**4** → **5**). Addition of two protons, followed by the cleavage of the oxygen−oxygen bond, results in the active iron-oxy species (**7**), also termed compound I, which rapidly oxidizes the substrate stereospecifically and regiospecifically by the transfer of the active oxygen atom. The hydroxylated product is released from the active site and the enzyme returns to its initial iron(III) resting state (**1**). At each step of the catalytic reaction cycle, knowledge about the electronic structure of the iron porphyrin, in particular the spin state of the iron center, is crucial for the understanding on how hemoproteins perform their biological functions.

---

* To whom correspondence should be addressed.

10.1021/jp0441442 CCC: $30.25

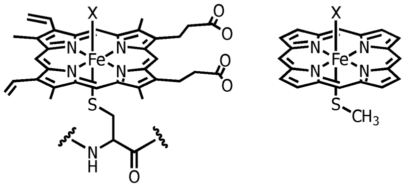

(a) (b)

X = OH_n	**1**	**1’**
X = none	**2**	**2’**

Figure 2. (a) Proto porphyrin IX (heme) with cysteine as axial ligand and (b) the model iron porphyrin with a mercaptide as axial ligand.

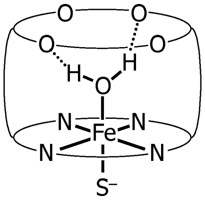

Figure 3. Crown-capped model prepared by Woggon et al.[19] The lower nitrogen containing ring represents the porphyrin ring and the upper one with oxygen atoms the crown-ether moiety.

In the resting state (**1**) of the catalytic reaction cycle, a water molecule is bound to the iron and forms the sixth ligand to the iron atom. This water molecule is displaced upon substrate binding (**2**). In both cases the heme iron atom is in the iron(III) state. With regard to the possible pairing of the five d electrons of the iron(III) center, three spin states are possible, that is a doublet, quartet, or sextet with respectively one, three, or five unpaired electrons. In native $P450_{cam}$, a change from hexacoordinated low-spin doublet iron(III) in **1** to pentacoordinated high-spin sextet iron(III) in the enzyme substrate complex **2** is observed experimentally.[22] Reduction of this second species gives rise to a pentacoordinated high spin quintet iron(II) complex **3**. It is this high spin iron(II) complex that is able to form a complex with triplet oxygen yielding the iron−dioxygen complex **4**, enabling the catalytic function. Therefore, the low-spin state of the resting state **1** is crucial for the function and efficiency of the P450 enzyme. This control mechanism prevents electrons to flow into the catalytic cycle if there is no bound substrate and hence suppresses uncoupling, that is, the formation of H_2O_2.[23]

The electronic ground states of the heme resting state (**1**) have been investigated computationally, using a variety of methods, for both mercaptide (CH_3S^-) and thiolate (HS^-) iron porphyrin model systems **1′** and **2′** (Figure 2).[14−21] Whereas the calculated relative energies between the low- and high-spin states differ markedly among these studies, with a significant dependence on the theoretical method and basis set, the low-spin doublet state is generally predicted to be the ground state for the resting state model in vacuo (**1′**).

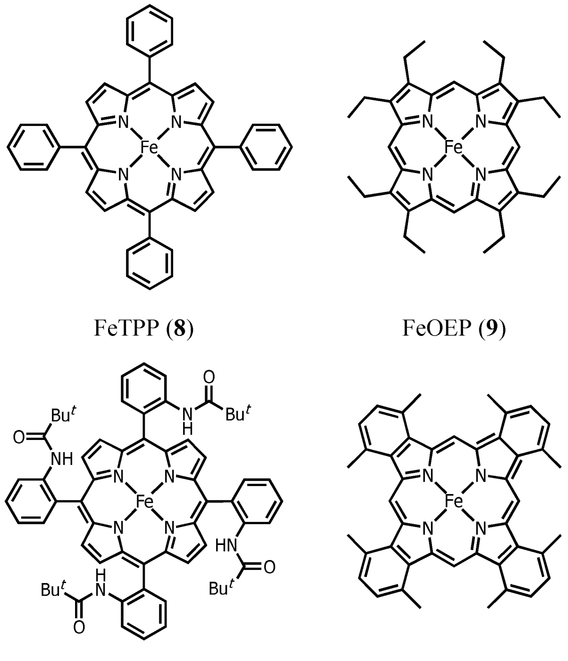

FeTPP (**8**) FeOEP (**9**)

FeTpivPP (**10**) FeOTBP (**11**)

Figure 4. Molecular structures of meso-tetraphenylporphyrin-iron(II) (FeTPP), octaethylporphyriniron(II) (FeOEP), picket-fence *meso*-tetrakis(α,α,α,α-*o*-pivalamidophenyl)porphyrin-iron(II) phthalocyanine (FeTpivPP), and octamethyl-tetrabenz-porphyrin-iron(II) (FeOTBP).

Besides the electronic ground state of the resting state, the nature of the sixth iron ligand appears also relevant.[4,5,14,18−27] For a synthetic model of **1**, it was shown that coordination of a water molecule to the iron(III) of the heme thiolate is insufficient to stabilize the low-spin state.[28] For water containing crown-capped iron porphyrins (Figure 3), synthesized to mimic the polarization of the cluster of six water molecules in the protein,[25] it was suggested that the ligated water molecule has, in fact, hydroxide ion character due to hydrogen bonding, thereby stabilizing the low-spin over the high spin state. This low spin ground state for the crown-capped resting state model is in accord with experiments of the protein and supports the explanation by Poulos et al.[24] that the low-spin resting state results from the induced hydroxide nature of the coordinated water due to the hydrogen-bonding network of the water cluster. H-bonding of iron(III) aqua porphyrin complex with the protein/sovent environment was also established in a recent B3LYP/CHARMM study by Schöneboom and Thiel.[5] In contrast, Goldfarb et al.[26,27] argued earlier that a plain water molecule is present as the sixth ligand to iron based on ^{17}O electron spin−echo envelope modulation spectroscopy (ESEEM) and electron−nuclear double resonance spectroscopy (ENDOR).

Noncoordinated iron(II) porphyrins have also been amply studied by various theoretical methods to resolve the relative stabilities of the singlet, triplet, and quintet states,[29−40] but in contrast to the iron(III) complex, they are inconclusive about the preferred ground state. Most DFT calculations predict an intermediate spin (triplet) state, but a high spin (quintet) state is preferred by electron correlation methods.[37−39] Because the unsubstituted iron porphyrin is not assessable, comparisons can only be made with experimental data of its derivatives, like meso-tetraphenylporphyrin **8** and iron(II) octaethylporphyrin **9** (Figure 4), for which triplet ground states have been proposed on the basis of their crystal structures, magnetic moments, Mössbauer spectra, and NMR contact shifts.[41−46] On the other hand, “picket fence” tetra(α,α,α,α-*o*-pivalamido-phenyl)-porphin-iron(II) **10** and octamethyl-tetrabenzporphyrin-iron(II) (**11**) both have a high spin iron(II) state, based on their reported magnetic moments.[47,48] However, solvation can be a determining factor. For example, on addition of pyridine or THF triplet iron(II)porphyrins, solvated in the noninteracting benzene, converts respectively to a pentacoordinated high spin or hexacoordinated low spin state.[49,50] A closer inspection into the nature of the various electronic states of the parent iron(II) porphyrin seems warranted.

In this context, it is relevant to explore in more detail whether DFT, the preferred method for sizable organometallic systems,[51,52] can predict reliably the relative energies of the various electronic states of iron(II) and iron(III) porphyrins. Particularly, the choice of functional is relevant. In a recent study on seven large iron complexes with experimentally known ground states, we showed the ability of DFT in calculating relative spin state energies (singlet to sextet) to be highly sensitive to the type of functionals.[53] For example, the frequently used functionals BLYP,[54,55] BP,[54,56] and PBE[57] do not predict the correct ground states for a number of iron complexes, whereas the newly developed GGA exchange functional OPTX[58] in combination with the PBE and Perdew correlation functionals, i.e., OPBE and OPerdew, perform excellently. In this paper, we use these two new functionals, emphasizing mainly OPBE, to scrutinize the electronic configurations of the unligated iron(II) and iron(III)porphyrins and their complexes with the thiolate and hydroxy ions and the water molecule.

Computational Details

Calculations were performed with the Amsterdam Density Functional (ADF) program.[59] The atomic orbitals on all atoms were described by an uncontracted triple-ζ valence plus polarization STO basis set (TZP). The inner cores of carbon, nitrogen, and oxygen ($1s^2$) and those of sulfur and iron ($1s^2$-$2s^2 2p^6$) were kept frozen. The exchange-correlation potential is based on the newly developed GGA exchange functional OPTX[58] in combination with the nonempirical PBE[57] (OPBE) and Perdew[56] correlation functionals (OPerdew). Geometries of all iron(II) and iron(III) porphyrins were optimized within C_{2v} symmetry (Figure 5) for the low, intermediate, and high spin states using the OPBE functional (see the Supporting Information). The OPBE and OPerdew SCF energies were calculated with an all-electron TZP basis set for all atoms.

To account for spin contamination, a correction based on the expectation value of S^2 calculated over de Kohn−Sham determinants is used even though these determinants are not eigenvalues of the S^2 operator. The spin projected energy E_s is then calculated by subtracting the energy contribution of the higher spin state E_{s+1} from the spin contaminated energy E_c with subsequent renormalization using eqs 1 and 2.[60]

$$a = \frac{\langle S^2 \rangle_c - s(s+1)}{\langle S^2 \rangle_{s+1} - s(s+1)} \tag{1}$$

$$E_s = \frac{E_c - aE_{s+1}}{1 - a} \tag{2}$$

Results and Discussion

Before focusing on the energetics of the species in the first steps of the catalytic cycle, we evaluate the relative energies of the three electronic states of both the iron(II) and iron(III) porphyrin. Next, the energetics of the ligated iron porphyrin moieties are considered. Their active sites are constructed by adding the axial ligands sequentially. Finally, the results of these active site models are evaluated for part of the catalytic cycle of cytochrome P450. Hence, the discussion uses a reversed order compared to **1**→**2**→**3**, which enables an analysis of the ligand effect. We start with the iron(II) complex, because it has received the most attention in the literature.

Iron(II) Porphyrin. Different electronic configurations are possible for each of its singlet, triplet, and quintet states depending on the occupation of six electrons over five transition metal d orbitals (d_{z^2}, $d_{x^2-y^2}$, d_{xy}, d_{xz}, and d_{yz}). Occupation numbers corresponding to the real Slater determinant are given in Table 1. For convenience, the electronic states are given symmetry labels associated with D_{4h} rather than the used C_{2v} symmetrical structure, because their geometrical differences are very small.

TABLE 1: Relative Energies (kcal mol^{-1}) of Different Electronic States of Iron(II) Porphyrin (C_{2v}) with Iron 3d Orbital Occupation Numbers

	Fe 3d orbital occupation					ΔE (kcal mol^{-1})	
	a_1	a_1	a_2	b_1	b_2		
state	d_{z^2}	$d_{x^2-y^2}$	d_{xy}	d_{xz}	d_{yz}	OPBE	OP[a]
singlet							
^1E_g	1.0	0.6	1.9	0.4	1.6	30.4[b]	30.3[b]
$^1A_{2g}$	1.8	0.6	1.9	1.0	1.0	33.2[b]	32.6[b]
$^1A_{1g}$(A)	0.1	0.6	1.9	1.9	1.9	35.9	36.4
$^1A_{1g}$(B)	1.8	0.6	1.9	0.4	1.6	39.3	38.5
triplet							
^3E_g(A)	1.0	0.7	1.9	1.7	1.0	0.0	0.0
$^3A_{2g}$	1.8	0.6	1.9	1.0	1.0	4.0	3.3
$^3B_{2g}$	1.0	0.8	1.0	1.8	1.8	5.3	5.4
^3E_g(B)	1.8	0.8	1.0	1.0	1.6	15.9	15.4
quintet							
^5E_g	1.0	1.3	1.0	1.1	1.8	6.3	6.5
$^5A_{1g}$	1.9	1.3	1.0	1.0	1.0	7.2	6.9
$^5B_{2g}$	1.0	1.2	1.9	1.0	1.0	12.7	13.0

[a] OPerdew. [b] Spin corrected energies.

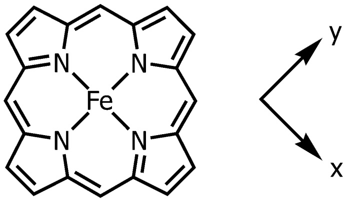

Figure 5. Atom labeling scheme for porphyrin (C_{2v}).

Table 1 also lists the related DFT relative energies for the OPBE and OPerdew functionals, whereas Table 2 gives these together with ab initio and DFT data reported in the literature.

The lowest energy structure of the iron(II) porphyrin, calculated with the OPBE functional, is a triplet state (^3E_g) that is favored over the lowest energy quintet (^5E_g) and the open shell singlet (^1E_g) states by 6.3 and 30.4 kcal mol^{-1}, respectively. The relative OPerdew energies are almost the same: the quintet ^5E_g and the singlet ^1E_g are respectively 6.5 and 30.3 kcal mol^{-1} higher in energy than triplet ^3E_g. This state ordering differs from that (quintet < triplet < singlet) obtained with the ab initio HF,[30] CI,[31] and CASSCF/CASPT2[37−39] methods (Table 2). The difference is attributable to the Hartree−Fock method that tends to underestimate the bonding between the metal and the ligand and to favor high spin configurations. In the high spin states, the antibonding $d_{x^2-y^2}$ orbital is occupied resulting in elongated Fe−N bonds. Hence, the ab initio CASSCF favored quintet state likely results from underestimating the Fe−N distances by both the basis set (cc-pVDZ) and the method (CASSCF).[61] To describe the quintet state accurately requires consideration of all Fe−N bonding interactions,[39] but the antibonding orbital is typically not included in the active space. Explicit accounting for non dynamical correlation with multireference Møller−Plesset (MRMP) and CASPT2 single-point energy calculations (using CASSCF geometries) do reduce the quintet−triplet energy difference, especially upon increasing the active space. Therefore, the question whether the quintet or triplet state is the ground state was still left open.[39]

All previous DFT calculations predict a triplet ground state, favoring either the ^3E_g (LDA, BP86) or $^3A_{2g}$ (BP86, B3LYP) electronic configuration depending on the used functionals with the largest energy difference amounting to 6.2 kcal mol^{-1} (Table 2). Quasirelativistic[62] and scalar relativistic zero-order regular approximations (ZORA)[63] have hardly an effect on the relative energies.[35,36] OPBE (OPerdew) gives a preference of the ^3E_g over the $^3A_{2g}$ state of 4.0 (3.3) kcal mol^{-1}, which, interestingly,

TABLE 2: Relative Energies (kcal mol^{-1}) for the Low-Lying Electronic States of Iron(II) Porphyrin

	singlet				triplet				quintet			
method	^1E_g	$^1A_{2g}$	$^1A_{1g}$(A)	$^1A_{1g}$(B)	^3E_g(A)	$^3A_{2g}$	$^3B_{2g}$	^3E_g(B)	^5E_g	$^5A_{1g}$	$^5B_{2g}$	ref
ab initio												
ROHF			67.5		35.4	28.0	48.2	68.5	5.5	0.0	8.3	[30]
			63.6	68.7	32.3	25.6	44	65	4.8	0.0	8.1	[31]
ROHF/CI			43.6	57.4	19.1	30.0	23.8	45	0.0	16.8	21.2	[31]
CASSCF(10/11)	64.1		58.8	66.9	32.1	31.5	43.7	59.0	4.6	0.0	7.2	[38]
(14/13)					22.3	20.0			3.1	0.0		[39]
(8/11)					11.7	9.3			5.5	0.0		[39]
CASPT2(10/11)	55.2		53.8	51.1	19.6	19.2	31.3	43.4	3.3	0.0	6.8	[38]
(14/13)					13.2	12.1			5.0	0.0		[39]
(8/11)					6.3	4.8			5.7	0.0		[39]
MRMP(10/11)	43.3		11.8	37.8	8.5	13.8	12.6	23.1	4.4	0.0	8.5	[37]
DFT												
MS-Xα/TZV			27.7		0.0	5.8	12.2	20.3	29.7	33.2	40.1	[32]
BH/DNP			28.4		0.0	4.4	13.4			35.5	40.5	[34]
BP86/TZP&DZP			31.1		0.0	1.4	7.4		24.9	25.4	30.7	[33]
BP86/TZP			31.4		1.8	0.0	5.1		17.8	15.5	21.9	[33]
			33.4		3.0	0.0	6.0	17.5	18.7	15.7	23.1	[36]
BP86/TZP; QR			34.4		2.8	0.0	6.0	17.1	19.6	16.4	24.2	[36]
BP86/TZP; ZORA			33.9		2.5	0.0	5.8	17.1	19.8	16.6	24.4	[36]
B3LYP/VTZ&6−31G(d)			37.1		6.2	0.0	14.3	21.2	12.5	6.9	17.8	[33]
OPBE/TZP	30.4	33.2	35.9	39.3	0.0	4.0	5.3	15.9	6.3	7.2	12.7	
OPerdew/TZP[a]	30.3	32.6	36.4	38.5	0.0	3.3	5.4	15.4	6.5	6.9	13.0	

[a] SCF energy of OPBE optimized geometry.

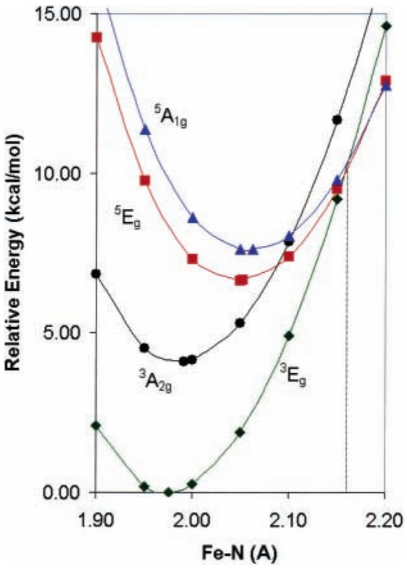

Figure 6. Relative energies of various electronic states of the optimized iron(II) porphyrin structure (C_{2v} symmetry) with respect to the distance (constrained) of two opposite iron−nitrogen distances.

TABLE 3: Relative Energies (kcal mol^{-1}) of Different Electronic States of Iron(III) Porphyrin (C_{2v}) with Iron 3d Orbital Occupation Numbers

	Fe 3d orbital occupation					ΔE (kcal mol^{-1})	
state	a_1 d_{z^2}	a_1 $d_{x^2-y^2}$	a_2 d_{xy}	b_1 d_{xz}	b_2 d_{yz}	OPBE	OPerdew
doublet							
$^2B_{2u}$[b]	1.0	0.8	1.0	1.8	1.8	23.2[a]	23.0[a]
^2E_g	1.9	0.7	1.9	0.7	1.1	34.4[a]	33.6[a]
$^2A_{1g}$	1.0	0.7	1.9	0.8	1.9	37.3[a]	37.1[a]
$^2A_{2g}$	1.0	0.8	1.9	1.3	1.3	40.5[a]	40.5[a]
quartet							
$^4A_{2g}$	1.0	0.8	1.9	1.2	1.2	0.0	0.0
$^4B_{1g}$	1.9	1.0	1.0	1.1	1.1	9.9	9.5
$^4A_{1u}$[c]	1.9	0.6	1.9	1.0	1.0	23.1	22.2
$^4A_{2u}$[d]	1.9	0.6	1.9	1.0	1.0	24.9	24.0
$^4B_{2u}$[d]	1.0	0.8	1.0	1.8	1.8	25.5	25.3
sextet							
$^6A_{1g}$	1.0	1.4	1.0	1.3	1.3	13.0	13.2

[a] Spin corrected energies. [b] Antiferromagnetic coupling of an electron in the a_{1u} orbital with the unpaired electrons of the iron center. [c] Ferromagnetic coupling of an electron in the a_{2u} orbital with the unpaired electrons of the iron center. [d] Ferromagnetic coupling of an electron in the a_{1u} orbital with the unpaired electrons of iron center.

contrasts the order obtained with BP86 and B3LYP. For iron(II) phthalocyanine, with an experimentally assigned ^3E_g triplet state,[64] OPBE (OPerdew) likewise favors the ^3E_g over the $^3A_{2g}$ state by 6.0 (5.2) kcal mol^{-1}. Noteworthy is that the modest OPBE (OPerdew) energy difference of the ^3E_g state with the two quintet states ^5E_g (6.3 (6.5) kcal mol^{-1}) and $^5A_{1g}$ (7.2, 6.9 kcal mol^{-1}) states, as compared with the other DFT calculations, is of a similar magnitude as the reported B3LYP preference for $^5A_{1g}$ over the other states.

To explore the sensitivity of the OPBE relative energies of these states to the geometry of the porphyrin (C_{2v}), we varied the core size, that is, the distance between the iron and the nitrogen atoms. As noted, elongation of the Fe−N distances favors the quintets because of the interaction of the antibonding metal $d_{x^2-y^2}$ with the nitrogen p_y orbitals of the porphyrin ring. The optimized bond distance for the ^3E_g, $^3A_{2g}$, ^5E_g, and $^5A_{1g}$ states are 1.98, 1.99, 2.05, and 2.06 Å, respectively. Figure 6 illustrates the dependence of the relative energy of these states on the Fe−N distance. The data show that within the experimentally observed Fe−N range of 1.97−2.07 Å, the triplet ^3E_g remains the ground state. The crossover to the quintet states (^5E_g and $^5A_{1g}$) occurs at the large Fe−N distance of 2.16 Å.

In summary, the OPBE calculations show ^3E_g to be the ground state of the iron(II) porphyrin, which concurs with available experimental observations.

Iron(III) Porphyrin. Oxidation of the iron(II) porphyrin yields the cationic iron(III) porphyrin species, i.e., the reverse of the reduction of **2** to **3**. Depending on the pairing of the five valence d electrons of the iron(III) center, a doublet, quartet, or sextet spin states results. The ground-state calculated with the OPBE functional is a quartet ($^4A_{2g}$) with a sextet ($^6A_{1g}$) 13.0 kcal mol^{-1} and a doublet state ($^2B_{2u}$) 23.2 kcal mol^{-1} higher in energy; the OPerdew energies are almost the same (Table 3). Thus, oxidation of triplet ^3E_g iron(II) porphyrin occurs by removal of one electron from the iron d_π orbital (d_{xz} or d_{yz}) to quartet $^4A_{2g}$ iron(III) complex. The relative order of the four

TABLE 4: Relative Energies (kcal mol^{-1}) for the Low-Lying Electronic States of Iron(III) Porphyrin

method	doublet			quartet			ref
	$^2B_{2u}$	^2E_g	$^4A_{2g}$	$^4B_{1g}$	$^4A_{1u}$	$^4A_{2u}$	
BP86/TZP		22.4	0.0	7.8	16.4	16.4	[65]
OPBE/TZP	23.2	34.4	0.0	9.9	23.1	24.9	

TABLE 5: Relative Energies (kcal mol^{-1}) of the Iron Porphyrin Species with Axial Thiolate (HS$^-$), Hydroxo (HO$^-$), and Aqua (H_2O) Ligands, Using Fully Optimized Structures

species	low spin		intermediate spin		high spin	
[Fe^{II}P]	28.9		0.0		6.3	
[Fe^{III}P]$^+$	26.4		0.0		13.0	
[HSFe^{II}P]-	6.7	(22.2)	5.2	(−5.2)	0.0	(6.3)
[HSFe^{III}P]	1.9	(24.5)	4.2	(−4.2)	0.0	(13.0)
[Fe^{II}POH]-	12.2	(16.7)	8.0	(−8.0)	0.0	(6.3)
[Fe^{III}POH]	9.8	(16.6)	6.2	(−6.2)	0.0	(13.0)
[Fe^{II}POH$_2$]	19.2	(9.7)	0.0	3.4	(2.9)	
[Fe^{III}POH$_2$]$^+$	26.6	(−0.2)	0.0	8.4	(4.6)	
[HSFe^{II}POH]$^{2-}$	0.0	(6.7)	0.2	(5.0)	-	
[HSFe^{III}POH]$^-$	0.0	(1.9)	12.0	(−7.8)	13.6	(−0.6)

[a] Values in parentheses indicate the relative (de)stabilization compared to the nonligated iron porphyrins. Those in italics are relative to the thiolate complexes.

quartet states is like that reported for the Becke-Perdew functional (Table 4).[65]

The lowest energy doublet $^2B_{2u}$ has three unpaired electrons, two of which are localized in the iron d orbitals in a triplet configuration, and the third electron in a porphyrin a_{1u} orbital that is coupled in an antiferromagnetic manner to the triplet iron pair. Ferromagnetic coupling gives quartet $^4B_{2u}$, which has nearly the same energy as doublet $^2B_{2u}$.

In summary, the relative energies for the different spin states of both the iron(II) and iron(III) porphyrins are similar, that is, intermediate spin < high spin < low spin.

P450 Active Site Models. So far, we have described the electronic states of the naked iron(II) and iron(III) porphyrins. In this section, we address those of the iron porphyrins ligated with thiolate and hydroxy anions and the water molecule. The HS$^-$ group is used as a mimic for the cysteine amino acid residue in the protein of cytochrome P450.

Thiolate iron(III) porphyrin complex [HSFe^{III}P] has a sextet ground state that is energetically favored over the doublet by a mere 1.9 kcal mol^{-1} and over the quartet by a modest 4.2 kcal mol^{-1} (Table 5). Nevertheless, HS$^-$ complexation gives a state change from intermediate to high spin. The same applies for iron(II) porphyrin, resulting in a quintet ground state for the thiolate complex that is preferred over the triplet and singlet by 5.2 and 6.7 kcal mol^{-1}, respectively. It is evident that the thiolate ligand reduces the energy differences between the electronic states of both the Fe(II) and Fe(III) porphyrins substantially due to the large relative stabilization of the low spin states (22.2 (Fe(II)) and 24.5 (Fe(III)) kcal mol^{-1}) with a concomitant modest destabilization of the intermediate spin states (5.2 (Fe(II)) and 4.2 (Fe(III)) kcal mol^{-1}), making them even competitive in the case of the Fe(II) complex (Table 5). Although the calculated relative energies of the various spin states of the HS$^-$ complexes concur with earlier DFT calculations, the OPBE functional gives the smaller energy differences (Table 6).[21]

The influence of the thiolate group is highlighted by the comparison with the HO$^-$ and H_2O ligands (Table 5). Like HS$^-$, ligation with HO$^-$ gives a preferred high spin state for both the Fe(II) and Fe(III) porphyrins, but more pronounced, because the relative stabilization for the low spin is much smaller (ca. 17 vs 23 kcal mol^{-1}) while the intermediate spin is slightly more destabilized (ca. 7 vs 5 kcal mol^{-1}). In sharp contrast to the major influence of these strong stabilizing anionic ligands on the electronic states, axial coordination by a neutral water molecule to either of the iron porphyrins has only a modest effect with the intermediate spin clearly remaining the preferred electronic state. Although the hydroxo ligand acts as strong σ- and π-donating ligand, the weak H_2O ligand does not change the relative ordering of the iron d orbitals. It follows that the negative charge stabilizes both the high and low spins, which is not surprising in light of the tighter interaction with the ligand, and this effect is strongest for the thiolate group because of its more polarizable sulfur atom.

TABLE 6: Relative OPBE Energies (kcal mol^{-1}) of the Thiolate Iron Porphyrin Species as Models for the Resting State (1), Substrate Bound State (2), and the First Reduced State (3) Optimized at DFT Level

species	method	R	relative energies, kcal mol^{-1}			ref
			LS[a]	IS[b]	HS[c]	
[RSFe^{III}P]	OPBE/TZP	H	1.9	4.2	0.0	
	B3LYP/LACVP[d]	H	4.2	4.2	0.0	[4]
	B3LYP/DZ[e]	Me	2.3	12.0	0.0	[21]
[RSFe^{II}P]$^-$	OPBE/TZP	H	6.7	5.2	0.0	
	B3LYP/LACV3P[d]	H	14.1	9.4	0.0	[4]
	B3LYP/DZ[e]	Me	11.3	7.6	0.0	[21]
[RSFe^{III}POH]$^-$	OPBE/TZP	H	0.0	12.0	13.6	
	B3LYP/DZ[g]	Me	0.0	13.0	11.1	[21]
[RSFe^{III}POH$_2$]	B3LYP/DZ[f]	Me	0.0		2.5	[19]
	B3LYP/DZ[g]	Me	0.4	13.8	0.0	[21]
	BP86/DZP+SZ[h,i]	H	0.0	13.5		[20]

[a] LS = low spin. [b] IS = intermediate spin. [c] HS = high spin. [d] LACVP(Fe) and 6-31G(H,C,N,S). [e] DZ(Fe) and 6-31G*(H,C,N,S). [f] pVDZ(Fe,N,O) and 3-21G*(H,C,S). [g] DZ(Fe), 6-31+G*(O), and 6-31G*(N,H,C,S). [h] DZVP2(Fe), 6-31G*(N,S,O), and STO-3G(C,H). [i] Optimized geometries with D_{4h} constraints for the porphyrin ring.

Having established that [HSFe^{III}P] prefers a sextet ground state in concurrence with the experimental studies on **2** of the catalytic cycle of P450, we next evaluate, by using this model, the nature of species **1**, the resting state for P450, that leads to **2**. We recall that it has been suggested, based on experimental studies, that water as part of a cluster of six molecules, possibly with anionic character, is coordinated to the iron. Therefore, we inspect the properties of the water and hydroxo ligated iron(III) porphyrins [HSFe^{III}POH$_2$] and [HSFe^{III}POH]$^-$, respectively, using fully optimized geometries for each spin state.

The aqua thiolate iron(III) porphyrin [HSFe^{III}POH$_2$] with its water molecule almost parallel to the porphyrin ring has a doublet ground state. There are two important aspects to this species, its geometry and its energy. Recently, Shaik and coworkers reported two conformations with the water molecule either “tilted” (parallel) or “upright” (orthogonal). They found the “tilted” form to be stabilized by hydrogen bonds between the water molecule and two of the nitrogen atoms of the porphyrin with, however, a very small energy difference of 1.1 kcal mol^{-1} over the “upright” form at B3LYP/LACVP(Fe);6-31G. At this level of theory, the “upright” form is a transition structure for planarization. At BP86/DZVP2(Fe);6-31G*(N,O,S);STO-3G(C,H) the difference in energy is much larger (6.6 kcal mol^{-1}), but a D_{4h} symmetry restriction was applied for the porphyrin ring. Using OPBE we did not obtain a minimum energy “upright” conformation. There are also other differences between the theoretical methods. Although OPBE gives a “tilted” minimum energy structure, the barrier for the

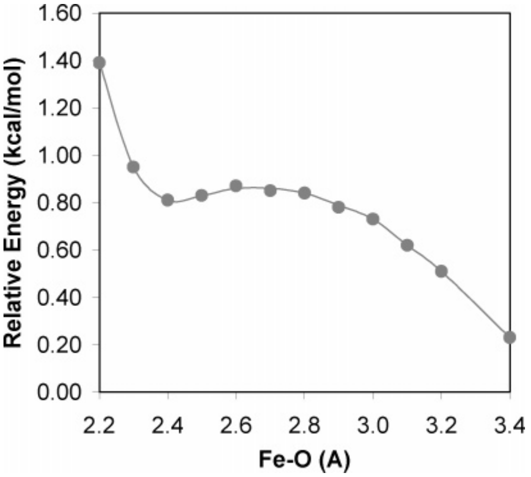

Figure 7. Relative energies of the thiolate aqua iron(III) porphyrin complex with respect to the distance (restrained) between the iron atom and the oxygen atom of the water molecule. The energetic valueas are with respect to the energy of the separate molecules.

4.2 kcal mol^{-1} exothermic dissociation of water to give sextet [HSFe^{III}P] amounts to a mere 0.06 kcal mol^{-1} (Figure 7), showing that the water molecule is essentially not bound. This result contrasts with the 3.5 kcal mol^{-1} favorable binding reported at B3LYP/DZ.[21] Thus, the binding of water to the iron center of [HSFe^{III}P] is rather sensitive to the theoretical method employed, an observation which is corroborated by a comparison of 53 different functionals used to calculate the H_2O binding energy for the OPBE optimized geometry of doublet [HSFe^{III}-POH$_2$] (see the Supporting Information).

BP86 calculations on partly optimized geometries (D_{4h} for the porphyrin ring) gave an energetic preference of 13.5 kcal mol^{-1} for the doublet over the quartet state, which has, however, an Fe−O bond distance of 8.204 Å showing that the water molecule is not bound; no sextet was described in this study. A B3LYP study reported a similar doublet-quartet energy difference for mercapto complex [CH$_3$SFe^{III}POH$_2$] but also showed the high spin state to be energetically favored over the doublet by 0.4 kcal mol^{-1}. Interestingly, the Fe−O bond distance for the sextet of 3.727 Å indicates that interaction of the water molecule with the porphyrin moiety in this high spin state is very weak. In fact, this situation is similar to the one we described for doublet [HSFe^{III}POH$_2$] calculated with OPBE. A related B3LYP study reported the quartet to be 2.5 kcal mol^{-1} less stable, but it used the geometry of the doublet. We were unable to obtain OPBE optimized geometries for the quartet and the sextet. In summary, the DFT calculations suggest that the water molecule is likely not bound to the porphyrin moiety of [RSFe^{III}P] and has at best a very weak interaction with the iron center.[66]

Instead, the hydroxy anion is tightly bound to the thiolate iron(III) porphyrin with a binding energy of 63.1 kcal mol^{-1} for the doublet ground state that is preferred over the quartet and sextet by 12.0 and 13.6 kcal mol^{-1}, respectively. Similar energy differences have been reported for the electronic states of the mercapto complex [CH$_3$SFe^{III}POH]$^-$.[21] Tight binding is expected as interaction of the anion with the electropositive iron enables dissipation of charge. However, the anionic complex is not likely to represent the resting state **1** of the cytochrome P450 catalytic cycle, because the OH$^-$ group is too tightly bound. On the other hand, protonation would afford aqua complex [HSFe^{III}POH$_2$], which, as discussed, is not stable and will release water to give high spin [HSFe^{III}P] that models the first active species in the catalytic cycle.

Alternatively, the aqua complex can be considered as one extreme and the hydroxo complex as the other. That is, if the water molecule does not only coordinate to the heme of cytochrome P450 but interacts also with the peptide backbone through hydrogen bonding, it effectively acts as a slightly basic ligand. Such a situation has been suggested in an experimental study on the crown-capped benzene-thiolate aqua iron porphyrin model (Figure 3) that incorporated a water cluster to mimick the resting state of the enzyme.[25] For this model, it was shown that removal of the water molecules by a camphor substrate changes the resting state from low to high spin. It has further been shown that lowering the pH induces a shift in substrate free cytochrome P450cam toward an increased high spin fraction.[67] The needed higher acidity is in line with breaking up the hydrogen bonds to enable detachment of water from the resting state to form the high spin active porphyrin complex.

It would appear that the amino acids of the peptide part of cytochrome P450 fulfill the important, established function to bind various (six) water molecules through a hydrogen-bonding network to induce some anionic character for one to coordinate favorably with the iron of the heme. This stabilization and simultaneous blocking of the heme site represents the resting state of the catalytic cycle. Disturbing the hydrogen-bonding network, for example, by introducing the substrate camphor in the heme pocket of P450cam, removes the anionic character and liberates the coordinated water molecule, which is no longer bound to the iron center, and simultaneously changes the electronic state from low to high spin, thereby activating the catalytic cycle. This interpretation is in line with a recent QM/MM study (B3LYP/CHARMM) on the resting state of P450cam that showed the importance of H-bond interactions of the axial water ligand within the binding pocket.[5]

Conclusions

This density functional theory study comprehensively evaluates the performance of the newly developed OPBE and OPerdew functionals against several commonly used ones (B3LYP, BP86, and others) and selected ab initio methods (CASSCF, CASSP2, and MRMP2) by calculating the relative energies of the various electronic states of both the iron(II) and the iron(III) porphyrins. It shows that both species have a clear preference for an intermediate spin as ground state, that is a triplet < quintet < singlet spin state ordering with ^3E_g favored over $^3A_{2g}$ for Fe(II) and a corresponding one, quartet < sextet < doublet, for the Fe(III) porphyrin.

Adding a thiolate anion to the Fe(II) and Fe(III) porphyrins, thereby mimicking cytochrome P450's heme with a cysteine amino acid residue, changes the preferred ground state for both species to high spin. The OPBE functional was used to evaluate the interaction of a water molecule and a hydroxy anion to the thiolate complexed Fe(III) porphyrin to model the resting state of the catalytic cycle of P450s. A low spin species is obtained in both cases, but the interaction of the iron center with the water molecule is repulsive, whereas the hydroxy anion is tightly bound. Hence, on protonating the HO$^-$ ligand, water will be formed and repelled from the heme to give a high spin Fe(III) complex. Alternatively and more likely, H_2O is part of a water cluster of six molecules, as in cytochrome P450cam, that interacts through H-bonding with the peptide part of the enzyme to induce anionic character. Disturbing the H-bonding network by, for example, introducing a substrate in the heme pocket of the P450 will remove the anionic character, repel the water molecule, and initiate the catalytic cycle.

Embedding the protein environment in the calculations is currently in progress using a new implementation of the QM/MM approach for the catalytic cycle of cytochromes P450s.

Acknowledgment. The Center of Complex Molecules of the Vrije Universiteit is acknowledged for financial support and the National Computing Facilities Foundation (NCF) for the use of their supercomputer facilities with financial support from The Netherlands Organization for Scientific Research (NWO).

Supporting Information Available: Cartesian coordinates and energies. This material is available free of charge via the Internet at http://pubs.acs.org.

References and Notes

(1) Lever, A. B. P.; Gray, H. B. *Iron Porphyrin*; Addison-Wesley: Reading, PA, 1983.

(2) Ortiz de Montellano, P. R., Ed. *Cytochrome P450: Structure, Mechanism and Biochemistry*, 2nd ed.; Plenum Press: New York, 1995.

(3) Sono, M.; Roach, M. P.; Coulter, E. D.; Dawson, J. H. *Chem. Rev.* **1996**, *96*, 2841−2888.

(4) Meunier, B.; de Visser, S. P.; Shaik S. *Chem. Rev.* **2004**, *104*, 3947−3980.

(5) Schöneboom, J. C.; Thiel, W. *J. Phys. Chem. B.* **2004**, *108*, 7468−7478.

(6) Newcomb, M.; Hollenberg P. F.; Coon, M. J. *Arch. Biochem. Biophys.* **2003**, *409*, 72−79.

(7) Guallar, V.; Friesner, R. A. *J. Am. Chem. Soc.* **2004** *126*, 8501−8508.

(8) Schöneboom, J. C.; Lin, H.; Reuter, N.; Thiel, W.; Cohen, S.; Ogliaro, F.; Shaik, S. *J. Am. Chem. Soc.* **2002**, *124*, 8142−8151.

(9) Schöneboom, J. C.; Cohen, S.; Lin, H.; Shaik, S.; Thiel, W. *J. Am. Chem. Soc.* **2004**, *126*, 4017−4034.

(10) Guallar, V.; Baik, M. H.; Lippard, S. J.; Friesner, R. A. *Proc. Natl. Acad. Sci. U.S.A.* **2003**, *100*, 6998−7002.

(11) Tyson, C. A.; Lipscomb, J. D.; Gunsalus, I. C. *J. Biol. Chem.* **1972**, *247*, 5777−5784.

(12) Yoshizawa, K.; Kamachi, T.; Shiota, Y. *J. Am. Chem. Soc.* **2001**, *123*, 9806−9816.

(13) Kamachi, T.; Yoshizawa, K. *J. Am. Chem. Soc.* **2003**, *125*, 4652−4661.

(14) Harris, D.; Loew, G. *J. Am. Chem. Soc.* **1993**, *115*, 8775−8779.

(15) Loew, G. H.; Harris, D. L. *Chem. Rev.* **2000**, *100*, 407−419.

(16) Göller, A. H.; Clark, T. *J. Mol. Struct.* **2001**, *541*, 263−281.

(17) de Groot, M. J.; Havenith; R. W. A.; Vinkers, H. M.; Zwaans, R.; Vermeulen, N. P. E.; van Lenthe, J. H. *J. Comput.-Aided Mol. Des.* **1998**, *12*, 183−193.

(18) Green, M. T. *J. Am. Chem. Soc.* **1998**, *120*, 10772−10773.

(19) Lochner, M.; Meuwly, M.; Woggon, W.-D. *Chem. Commun.* **2003**, *12*, 1330−1332.

(20) Filatov, M.; Harris, N.; Shaik, S. *J. Chem. Soc., Perkin Trans. 2* **1999**, 399−410.

(21) Rydberg, P.; Sigfridsson, E.; Ryde, U. *J. Biol. Inorg. Chem.* **2004**, *9*, 203−223.

(22) Sligar, S. G., *Biochemistry* **1976**, *15*, 5399−5406.

(23) Mueller, E. J.; Loida, P. J.; Sligar, S. G. In *Cytochrome P450: Structure, Mechanism and Biochemistry*, 2nd ed.; Ortiz de Montellano, P. R., Ed.; Plenum Press: New York, 1995; pp 83−124.

(24) Raag, R.; Poulos, T. L. *Frontiers in Biotransformation*; Ruckpaul, K., Rein, H., Eds.; Akademie Verlag: Berlin, 1992; Vol. 7, pp 1−43.

(25) Lochner, M.; Mu, L.; Woggon, W.-D. *Adv. Synth. Catal.* **2003**, *245*, 743−765.

(26) Goldfarb, D.; Bernardo, M.; Thomann, H.; Kroneck, P. M. H.; Ullrich, V. *J. Am. Chem. Soc.* **1996**, *118*, 2686−2693.

(27) Thomann, H.; Bernardo, M.; Goldfard, D.; Kroneck, P. M. H.; Ullrich, V. *J. Am. Chem. Soc.* **1995**, *117*, 8243−8251.

(28) Aissaoui, H.; Bachmann, R.; Schweiger, A.; Woggon, W.-D. *Angew. Chem., Int. Ed. Engl.* **1998**, *37*, 2998−3002.

(29) Edwards, W. D.; Weiner, B.; Zerner, M. C. *J. Am. Chem. Soc.* **1986**, *108*, 2196−2204.

(30) Obara, S.; Kashiwagi, H. *J. Chem. Phys.* **1982**, *77*, 3155−3165.

(31) Rawlings, D. C.; Gouterman, M.; Davidson, E. R.; Feller, D. *Int. J. Quantum Chem.* **1985**, *28*, 773−796.

(32) Delley, B. *Physica B* **1991**, *172*, 185−193.

(33) Kozlowski, P. M.; Spiro, T. G.; Bérces, A.; Zgierski, M. Z. *J. Phys. Chem. B* **1998**, *102*, 2603−2608.

(34) Matsuzawa, N.; Ata, M.; Dixon, D. A. *J. Phys. Chem.* **1995**, *99*, 7698−7706.

(35) Liao, M.-S.; Scheiner, S. *J. Chem. Phys.* **2002**, *116*, 3635−3645.

(36) Liao, M.-S.; Scheiner, S. *Chem. Phys.* **2002**, *285*, 195−206.

(37) Choe, Y.-K.; Hashimoto, T.; Nakano, H.; Hirao, K. *Chem. Phys. Lett.* **1998**, *295*, 380−388.

(38) Choe, Y.-K.; Nakajima, T.; Hirao, K. *J. Chem. Phys.* **1999**, *111*, 3837−3845.

(39) Pierloot, K. *Mol. Phys.* **2003**, *101*, 2083−2094.

(40) Oliveira, K. M. T.; Trsic, M. *J. Mol. Struct. (THEOCHEM)* **2001**, *539*, 107−117.

(41) Collman, J. P.; Reed, C. A. *J. Am. Chem. Soc.* **1973**, *95*, 2048−2049.

(42) Collman, J. P.; Hoard, J. L.; Kim, N.; Lang, G.; Reed, C. A. *J. Am. Chem. Soc.* **1975**, *97*, 2676−2681.

(43) Goff, H.; La Mar, G. N.; Reed, C. A. *J. Am. Chem. Soc.* **1977**, *99*, 3641−3646.

(44) Boyd, P. D. W.; Buckingham, D. A.; McMeeking, R. F.; Mitra, S. *Inorg. Chem.* **1979**, *18*, 3585−3591.

(45) Dolphin, D.; Sams, J. R.; Tsin, T. S.; Wong, K. L. *J. Am. Chem. Soc.* **1976**, *98*, 6970−6975.

(46) Strauss, S. H.; Silver, M. E.; Long, K. M.; Thompson, R. G.; Hudgens, R. A.; Spartalian, K.; Ibers, J. A. *J. Am. Chem. Soc.* **1985**, *107*, 4207−4215.

(47) Collman, J. P.; Gagne, R. R.; Reed, C. A.; Halbert, T. R.; Lang, G.; Robinson, W. T. *J. Am. Chem. Soc.* **1975**, *97*, 1427−1439.

(48) Sams, J. R.; Tsin, T. B. *Chem. Phys. Lett.* **1974**, *25*, 599−601.

(49) Brault, D.; Rougee, M. *Biochemistry* **1974**, *13*, 4591−4597.

(50) Brault, D.; Rougee, M. *Biochemistry* **1974**, *13*, 4598−4602.

(51) Rosa, A. M., Ph.D. Thesis, Department of Chemistry, Vrije Universiteit Amsterdam, The Netherlands, 1993.

(52) Baerends, E. J.; Ricciardi, G.; Rosa, A.; van Gisbergen, S. J. A. *Coord. Chem. Rev.* **2002**, *230*, 5−27.

(53) Swart, M.; Groenhof, A. R.; Ehlers, A. W.; Lammertsma K. *J. Phys. Chem. A* **2004**, *108*, 5479−5483.

(54) Becke, A. D. *Phys. Rev. A* **1988**, *38*, 3098−3100.

(55) Lee, C.; Yang, W.; Parr, R. G. *Phys. Rev. B* **1988**, *37*, 785−789.

(56) Perdew, J. P. *Phys Rev. B* **1986**, *33*, 8822−8824. Erratum. *Phys Rev. B* **1986**, *34*, 7406.

(57) Perdew, J. P.; Burke, K.; Ernzerhof, M. *Phys Rev. Lett* **1996**, *77*, 3865−3868.

(58) Handy, N. C.; Cohen, A. J. *Mol. Phys.* **2001**, *99*, 403−412.

(59) ADF version 2004.01. See also: te Velde, G.; Bickelhaupt, F. M.; Baerends, E. J.; Fonseca Guerra, C.; van Gisbergen, S. J. A.; Snijders, J. G.; Ziegler, T. *J. Comput. Chem.* **2001**, *22*, 931.

(60) Wittbrodt, J. M.; Schlegel, H. B. *J. Chem. Phys.* **1996**, *105*, 6574−6577.

(61) Pierloot, K.; Persson, B. J.; Roos, B. O. *J. Phys. Chem.* **1995**, *99*, 3465−3472.

(62) Ziegler, T.; Tschinke, V.; Baerends, E. J.; Snijders, J. G.; Ravenek, W. *J. Phys. Chem.* **1989**, *93*, 3050−3056.

(63) Van Lenthe, E.; Baerends, E. J.; Snijders, J. G. *J. Chem. Phys.* **1994**, *101*, 9783−9792.

(64) Coppens, P.; Li, L. *J. Chem. Phys.* **1984**, *81*, 1983−1993.

(65) Liao, M.-S.; Scheiner, S. *J. Chem. Phys.* **2002**, *117*, 205−219.

(66) For the used TZP basis set, the basis set superposition error (BSSE) is small (0.70 kcal mol^{-1}), whereas this error is rather large (6.20 kcal mol^{-1}) when a basis set of double-ζ (DZ) is used.

(67) Sligar, S. G.; Gunsalus, I. C. *Biochemistry* **1979**, *11*, 2290−2295.